
Non-Parametric Calibration for Classification

Jonathan Wenger

Technical University of Munich (TUM)
KTH Royal Institute of Technology
j.wenger@tum.de

Hedvig Kjellström

KTH Royal Institute of Technology
hedvig@kth.se

Rudolph Triebel

Technical University of Munich (TUM)
German Aerospace Center (DLR)
trieb@in.tum.de

Abstract

Many applications for classification methods not only require high accuracy but also reliable estimation of predictive uncertainty. However, while many current classification frameworks, in particular deep neural network architectures, provide very good results in terms of accuracy, they tend to underestimate their predictive uncertainty. In this paper, we propose a method that corrects the confidence output of a general classifier such that it approaches the true probability of classifying correctly. This classifier calibration is, in contrast to existing approaches, based on a non-parametric representation using a latent Gaussian process and specifically designed for multi-class classification. It can be applied to any classification method that outputs confidence estimates and is not limited to neural networks. We also provide a theoretical analysis regarding the over- and underconfidence of a classifier and its relationship to calibration. In experiments we show the universally strong performance of our method across different classifiers and benchmark data sets in contrast to existing classifier calibration techniques.

1 Introduction

With the recent achievements in machine learning, in particular in the area of deep learning, the range of applications for learning methods has also increased significantly. Especially in challenging fields such as computer vision or speech recognition, important advancements have been made using powerful and complex network architectures, trained on very large data sets. Most of these techniques are used for classification tasks, e.g. object recognition. We also consider classification in our work. However, in addition to achieving high classification accuracy, our goal is to also provide reliable uncertainty estimates for predictions. This is of particular relevance in safety-critical applications [1], such as autonomous driving and robotics. Reliable uncertainties can be used to increase a classifier's precision by reporting only class labels that are predicted with low uncertainty or for information theoretic analyses of what was learned and what was not. The latter is especially interesting in the context of active learning [2], where the learner actively selects the most relevant data samples for training via a query function based on the posterior predictive uncertainty of the model.

Unfortunately, current probabilistic classification approaches that inherently provide good uncertainty estimates, such as Gaussian processes, often suffer from a lower accuracy and a higher computational complexity on high-dimensional classification tasks compared to state-of-the-art convolutional neural network (CNN) architectures. It was recently observed that many modern CNNs are overconfident [3] and miscalibrated [4]. Here, calibration refers to adapting the confidence output of a classifier such that it matches its true probability of being correct. Originally developed in the context of forecasting

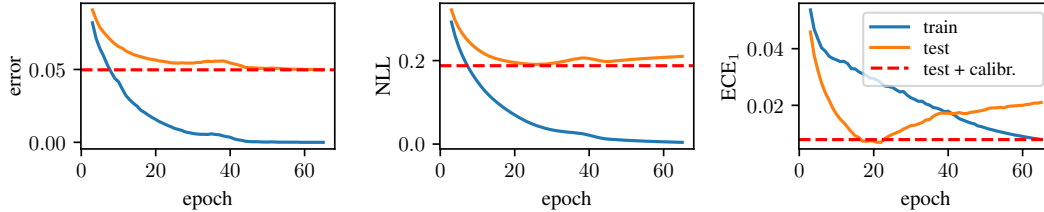


Figure 1: **Motivating example for calibration.** We trained a neural network with one hidden layer on MNIST [18] and computed the classification error, the negative log-likelihood (NLL) and the expected calibration error (ECE_1) over training epochs. We observe that while accuracy continues to improve on the test set, the ECE_1 increases after 20 epochs. Note that this is different from classical overfitting, as the test error continues to decrease. This shows that training and calibration need to be considered independently. This can be mitigated by post-hoc calibration using our method (dashed red line). The uncertainty estimation is improved with maintained classification accuracy.

[5, 6], uncertainty calibration has seen increased interest in recent years [4, 7–10], partly because of the popularity of CNNs which lack inherent uncertainty representation. Earlier studies show that also classical methods such as decision trees, boosting, SVMs and naive Bayes classifiers tend to be miscalibrated [11–13, 7]. Therefore, we claim that training and calibrating a classifier can be two different objectives that need to be considered separately, as shown in a toy example in Figure 1. Here, a simple neural network continually improves its accuracy on the test set during training, but eventually overfits in terms of NLL and calibration error. A similar phenomenon was observed in [4] for more complex models. Calibration methods perform a post-hoc improvement to uncertainty estimation using a small subset of the training data. Our goal in this paper is to develop a *multi-class calibration method for arbitrary classifiers*, to provide reliable predictive uncertainty estimates in addition to maintaining high accuracy.

We note that in contrast to recent approaches which strive to improve uncertainty estimation only for neural networks, including Bayesian neural networks [14, 15] and Laplace approximations (LA) [16, 17], our aim is a framework that is not based on tuning a specific classification method. This has the advantage that the method operates independently of the training process of the classifier and does not rely on training-specific values such as the curvature of the loss function as in LA methods.

Contribution In this work we demonstrate that popular classification models in computer vision and robotics are often not calibrated. We develop a new multi-class and model-agnostic approach to calibration, based on Gaussian processes, which have a number of desirable properties making them suitable as a calibration tool. Further, we study the relationship between active learning and calibration from a theoretical and empirical perspective.

Related Work Estimation of uncertainty, in particular in deep learning [19], is of considerable interest in the machine learning community at the moment. There are two main approaches in classification. First, by defining a model and loss function which inherently learns a good representation and second, by post-hoc calibration methods which transform output of the underlying model. Pereyra et al. [20] propose penalizing low entropy output distributions, Kumar et al. [9] suggest a trainable measure of calibration as a regularizer and Maddox et al. [21] employ an approximate Bayesian inference technique using stochastic weight averaging. Further, Milios et al. [22] approximate Gaussian process classifiers, which tend to have good uncertainty estimates by GP regression on transformed labels for improved scalability. Research on calibration goes back to statistical forecasting [5, 6] and approaches to provide uncertainty estimates for non-probabilistic binary classifiers [23–25]. More recently, Bayesian Binning into Quantiles [7] and Beta calibration [8] for binary classification and temperature scaling [4] for multi-class problems were proposed. Guo et al. [4] also discovered that modern CNN architectures do not provide calibrated output. A theoretical framework for evaluating calibration in classification was suggested by Vaicenavicius et al. [10]. Calibration was also previously considered in the online setting with potentially adversarial input [26]. Calibration in a broader sense is also of interest outside of the classification setting, e.g. in regression [27, 28], in the discovery of causal Bayesian network structure from observational data [29] and in the algorithmic fairness literature [30, 31].

2 Background

Notation Consider a data set $\mathcal{D} = \{(\mathbf{x}_n, y_n)\}_{n=1}^N$ assumed to be independent and identically distributed realizations of the random variable $(X, Y) \in \mathcal{X} \times \mathcal{Y}$ with $K = |\mathcal{Y}|$ labels. If not otherwise indicated any expectations are taken with respect to (X, Y) . Let $f : \mathcal{X} \rightarrow \mathbb{R}^K$ be a classifier with output $\mathbf{z} = f(\mathbf{x})$, prediction $\hat{y} = \arg \max_i(z_i)$ and associated confidence score $\hat{z} = \max_i(z_i)$. We define a calibration method $v : \mathbb{R}^K \rightarrow \mathbb{R}^K$ and denote its output by $\mathbf{p} = v(\mathbf{z})$.

2.1 Calibration

A classifier is called *calibrated* if its confidence in its class prediction matches the probability of its prediction being correct:

$$\mathbb{E}[1_{\hat{y}=y} \mid \hat{z}] = \hat{z}.$$

In order to measure calibration, we define the *expected calibration error* [7] for $1 \leq p < \infty$ by

$$\text{ECE}_p = \mathbb{E}[|\hat{z} - \mathbb{E}[1_{\hat{y}=y} \mid \hat{z}]|^p]^{\frac{1}{p}} \quad (1)$$

and the *maximum calibration error* [7] by $\text{ECE}_\infty = \max_{z \in [0,1]} |\hat{z} - \mathbb{E}[1_{\hat{y}=y} \mid \hat{z} = z]|$. In practice, we estimate the calibration error by using a fixed binning for \hat{z} as described in [7]. However, calibration is not sufficient for useful uncertainty estimates. A classifier on a balanced binary classification problem which always predicts probability 0.5 is perfectly calibrated, as its confidence matches the probability of making a correct prediction. Intuitively, we would like the probabilities of a prediction to be sufficiently close to 0 and 1 for them to be informative. Variations of this notion are known as sharpness or refinement [6, 32, 33].

2.2 Over- and Underconfidence

The notions of *over-* and *underconfidence*, originally introduced in the context of active learning [34], measure the average confidence of a classifier on its false predictions and the average uncertainty on its correct predictions, respectively:

$$o(f) = \mathbb{E}[\hat{z} \mid \hat{y} \neq y] \quad u(f) = \mathbb{E}[1 - \hat{z} \mid \hat{y} = y].$$

We show that there is a direct link between calibration and the two notions.

Theorem 1 (Calibration, Over- and Underconfidence)

Let $1 \leq p < q \leq \infty$, then the following relationship between over-, underconfidence and the expected calibration error holds:

$$|o(f)\mathbb{P}(\hat{y} \neq y) - u(f)\mathbb{P}(\hat{y} = y)| \leq \text{ECE}_p \leq \text{ECE}_q.$$

For a proof we refer to Section S1 of the supplementary material. We see that the expected calibration error bounds the weighted absolute difference of over- and underconfidence. In case of perfect calibration, the odds of making a correct prediction equal the ratio between over- and underconfidence. Similar results were established previously in the fairness literature [30, 31], where over- and underconfidence were termed generalized false positive and negative rates.

2.3 Calibration Methods

Calibration methods transform the output of a classifier and are fit on a typically significantly smaller hold-out set of the training data, which we call the calibration data set. In the following, we introduce the most prevalent methods.

2.3.1 Binary Calibration

Platt Scaling Originally introduced in order to provide probabilistic output for SVMs, Platt Scaling [23, 24] is a parametric calibration method. A logistic regression is fit to the confidence scores such that

$$v(\mathbf{z})_1 = (1 + \exp(-a\mathbf{z}_1 - b))^{-1}$$

for $a, b \in \mathbb{R}$. This parametric assumption is justified if the scores of each class are normally distributed with identical variance [35].

Isotonic Regression Isotonic regression [25] is a non-parametric approach. It assumes a non-decreasing relationship $v(\mathbf{z})_1 = m(z_1) + \varepsilon$ between the model confidence of the positive class and its probability of being correct. The piece-wise constant isotonic function m is found by minimizing a squared loss function.

Beta Calibration Beta calibration [8] was specifically designed for probabilistic classifiers with output range $z_1 \in [0, 1]$. A family of calibration maps is defined based on the likelihood ratio between two Beta distributions. The calibration map is given by

$$v(\mathbf{z})_1 = \left(1 + \exp(-c) \frac{(1 - z_1)^b}{z_1^a} \right)^{-1},$$

where $a, b, c \in \mathbb{R}$ are parameters to be fit on the calibration set.

Bayesian Binning into Quantiles BBQ [7] scores multiple equal-frequency binning models and uses a score weighted average of the accuracy in each bin as a calibration map. A binning model M is weighted by $P(M)P(\mathcal{D} | M)$, where $P(M)$ is uniform and the marginal likelihood $P(\mathcal{D} | M)$ can be computed in closed form given parametric assumptions on the data generation process.

2.3.2 Multi-class Calibration

One-vs-All In order to extend binary calibration methods to multi-class problems, Zadrozny and Elkan [25] suggest a one-vs-all approach, training a binary classifier on each split and calibrating subsequently. As most modern classifiers are inherently multi-class, this approach is not feasible anymore. We instead use a one-vs-all approach for the output \mathbf{z} of the multi-class classifier, train a calibration method on each split and average their predictions.

Temperature Scaling Temperature scaling [4] was introduced as a multi-class extension to Platt scaling for neural networks. For an output logit vector \mathbf{z} of a neural network and a *temperature* parameter $T > 0$, the calibrated confidence is defined as

$$v(\mathbf{z}) = \frac{\exp\left(\frac{z_j}{T}\right)}{\sum_{k=1}^K \exp\left(\frac{z_k}{T}\right)}. \quad (2)$$

The parameter T is determined by optimizing the NLL. By construction, the accuracy of the classifier is unchanged after scaling. Variants of this method known as vector and matrix scaling where the factor is replaced by a multi-dimensional affine map have proven ineffective.

3 Gaussian Process Calibration

We outline our non-parametric calibration approach in the following. Our aim is to develop a calibration method, which is inherently *multi-class*, suitable for *arbitrary classifiers*, makes as few assumptions as possible on the shape of the calibration map and can take prior knowledge into account. These desired properties readily lead to our approach using a latent Gaussian process [36].

Definition Assume a one-dimensional Gaussian process prior over the latent function $f(\mathbf{z})$, i.e. $f \sim \mathcal{GP}(\mu(\cdot), k(\cdot, \cdot | \theta))$ with mean function μ , kernel k and kernel parameters θ . Further, let the calibrated output be given by the *softargmax* inverse link function applied to the latent process evaluated at the model output

$$v(\mathbf{z})_j = \sigma(f(\mathbf{z}))_j = \frac{\exp(f(\mathbf{z}_j))}{\sum_{k=1}^K \exp(f(\mathbf{z}_k))}. \quad (3)$$

Note the similarity to multi-class Gaussian process classification, but in contrast we consider one shared latent function applied to each component of \mathbf{z} individually instead of K latent functions. We use the categorical likelihood

$$\text{Cat}(y | \sigma(f(\mathbf{z}))) = \prod_{k=1}^K \sigma(f(\mathbf{z}))_k^{[y=k]} \quad (4)$$

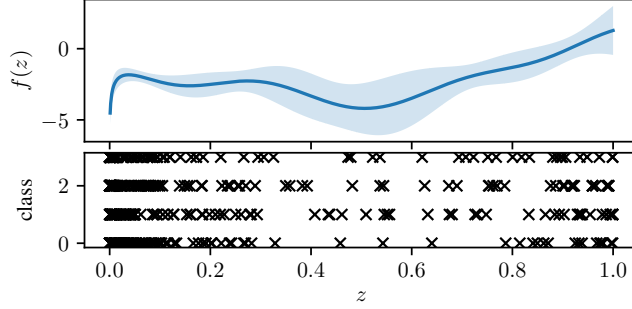


Figure 2: **Multi-class calibration using a latent Gaussian process.** Top: Latent function of multi-class GP calibration with prior mean $\mu(z) = \log(z)$ on a synthetic calibration data set with four classes and 100 calibration samples. Bottom: Input confidence and labels of the calibration data.

to obtain a prior on the class prediction. Making the prior assumption that the given classifier is calibrated and no further calibration is necessary corresponds to either $\mu(z) = \log(z)$ if the inputs are confidence estimates, or to the identity function $\mu(z) = z$ if the inputs are logits. The formulation is inspired by temperature scaling defined in (2). We replace the linear map by a Gaussian process to allow for a more flexible calibration map able to incorporate prior knowledge concerning its shape. An example of a latent function for a synthetic data set is shown in Figure 2. If the latent function f is monotonically increasing in its domain, the *accuracy of the underlying classifier is unchanged*.

Inference In order to infer the calibration map, we need to fit the underlying Gaussian process based on the confidence predictions or logits and ground truth classes in the calibration set. By our choice of likelihood, the posterior is not analytically tractable. In order for our method to scale to large data sets we only retain a sparse representation of the input data, making inference of the latent Gaussian process computationally less intensive. We approximate the posterior through a scalable variational inference method [37]. The joint distribution of the data (Z, \mathbf{y}) and latent variables \mathbf{f} is given by

$$p(\mathbf{y}, \mathbf{f}) = p(\mathbf{y} | \mathbf{f})p(\mathbf{f}) = \prod_{n=1}^N p(y_n | f_n)p(\mathbf{f}) = \prod_{n=1}^N \text{Cat}(y_n | \sigma(f_n))\mathcal{N}(\mathbf{f} | \mu, \Sigma_f),$$

where $\mathbf{y} \in \{1, \dots, K\}^N$, $\mathbf{f} = (f_1, f_2, \dots, f_N)^\top \in \mathbb{R}^{NK}$ and $f_n = (f(z_{n1}), \dots, f(z_{nK}))^\top \in \mathbb{R}^K$. The covariance matrix Σ_f has block-diagonal structure by independence of the calibration data. If performance is critical, a further diagonal assumption can be made. Note that we drop the explicit dependence on Z and θ throughout to lighten the notation. We want to compute the posterior $p(\mathbf{f} | \mathbf{y})$. In order to reduce the computational complexity from $\mathcal{O}((NK)^3)$, we define M inducing inputs $\mathbf{w} \in \mathbb{R}^M$ and inducing variables $\mathbf{u} \in \mathbb{R}^M$. The joint distribution is given by

$$p(\mathbf{f}, \mathbf{u}) = \mathcal{N} \left(\begin{bmatrix} \mathbf{f} \\ \mathbf{u} \end{bmatrix} \middle| \begin{bmatrix} \boldsymbol{\mu}_f \\ \boldsymbol{\mu}_u \end{bmatrix}, \begin{bmatrix} \Sigma_f & \Sigma_{f,u} \\ \Sigma_{f,u}^\top & \Sigma_u \end{bmatrix} \right). \quad (5)$$

Using Bayes' theorem the joint can be factorized as $p(\mathbf{y}, \mathbf{f}, \mathbf{u}) = p(\mathbf{y} | \mathbf{f})p(\mathbf{f} | \mathbf{u})p(\mathbf{u})$. We aim to find a variational approximation $q(\mathbf{u}) = \mathcal{N}(\mathbf{u} | m, S)$ to the posterior $p(\mathbf{u} | \mathbf{y})$. For general treatments on variational inference we refer interested readers to [38, 39]. We find the variational parameters m and S , the locations of the inducing inputs \mathbf{w} and the kernel parameters θ by optimizing a lower bound to the marginal log-likelihood

$$\begin{aligned} \log p(\mathbf{y}) &\geq \text{ELBO}(q(\mathbf{u})) \\ &= \mathbb{E}_{q(\mathbf{u})} [\log p(\mathbf{y} | \mathbf{u})] - \text{KL}[q(\mathbf{u}) || p(\mathbf{u})] \\ &\geq \mathbb{E}_{q(\mathbf{u})} [\mathbb{E}_{p(\mathbf{f} | \mathbf{u})} [\log p(\mathbf{y} | \mathbf{f})]] - \text{KL}[q(\mathbf{u}) || p(\mathbf{u})] \\ &= \mathbb{E}_{q(\mathbf{f})} [\log p(\mathbf{y} | \mathbf{f})] - \text{KL}[q(\mathbf{u}) || p(\mathbf{u})] \\ &= \sum_{n=1}^N \mathbb{E}_{q(f_n)} [\log p(y_n | f_n)] - \text{KL}[q(\mathbf{u}) || p(\mathbf{u})], \end{aligned} \quad (6)$$

where $q(\mathbf{f}) := \int p(\mathbf{f} | \mathbf{u})q(\mathbf{u}) d\mathbf{u}$ is Gaussian and only its K -dimensional marginals $q(f_n) = \mathcal{N}(f_n | \varphi_n, C_n)$ are required to compute the expectation terms. To do so, we make a second order Taylor approximation to $\log p(y_n | f_n)$ and obtain

$$\mathbb{E}_{q(f_n)} [\log p(y_n | f_n)] \approx \log p(y_n | \varphi_n) + \frac{1}{2} (\sigma(\varphi_n)^\top C_n \sigma(\varphi_n) - \text{diag}(C_n)^\top \sigma(\varphi_n)) \quad (7)$$

which can be computed in $\mathcal{O}(K^2)$. Computing the KL-divergence term in (6) is in $\mathcal{O}(M^3)$. Therefore, computing the objective (6) has complexity $\mathcal{O}(NK^2 + M^3)$. Note that this can be remedied through parallelization as all N expectation terms can be computed independently. The optimization can be performed either by using a gradient-based optimizer or as in our case by automatic differentiation. We refer to Section S2 of the supplementary material for a more detailed treatment of inference.

Prediction Given the approximate posterior $p(\mathbf{f}, \mathbf{u} | \mathbf{y}) \approx p(\mathbf{f} | \mathbf{u})q(\mathbf{u})$, predictions at new inputs Z_* are obtained via

$$p(\mathbf{f}_* | \mathbf{y}) = \int p(\mathbf{f}_* | \mathbf{f}, \mathbf{u})p(\mathbf{f}, \mathbf{u} | \mathbf{y}) d\mathbf{f}d\mathbf{u} \approx \int p(\mathbf{f}_* | \mathbf{u})q(\mathbf{u}) d\mathbf{u}$$

which is Gaussian. Means and variances of a latent value $\mathbf{f}_* \in \mathbb{R}^K$ can be computed in $\mathcal{O}(KM^2)$. The class prediction \mathbf{y}_* is then obtained by evaluating the integral

$$p(\mathbf{y}_* | \mathbf{y}) = \int p(\mathbf{y}_* | \mathbf{f}_*)p(\mathbf{f}_* | \mathbf{y}) d\mathbf{f}_*$$

via Monte-Carlo integration. While inference and prediction have higher computational cost than in other calibration methods, it is comparatively small to the training time of the underlying classifier, since usually only a small fraction of the data is necessary for calibration. Furthermore, calibration can be performed in parallel to training in the online setting.

4 Experiments

We experimentally evaluate our approach against the calibration methods presented in Section 2.3, applied to different classifiers on a range of binary and multi-class computer vision benchmark data sets. Besides convolutional neural networks, we are also interested in ensemble methods such as boosting and forests. All methods and experiments were implemented in Python 3.6 using the authors' original code, if available. Our GP-based method was implemented using `gpf1ow` [40] with a log mean function and a sum kernel consisting of an RBF and a white noise kernel.¹ We report the average ECE_1 estimated with 100 bins over 10 Monte-Carlo cross validation runs. We used the following data sets with indicated train, calibration and test splits:

- KITTI [41, 42]: Stream-based urban traffic scenes with features [43] from segmented 3D point clouds. 8 or 2 classes, dimension 60, train: 16000, calibration: 1000, test: 8000.
- PCam [44]: Detection of metastatic tissue in histopathologic scans of lymph node sections conv. to gray scale. 2 classes, dimension 96×96 , train: 22768, calibration: 1000, test: 9000.
- MNIST [18]: Handwritten digit recognition. 10 classes, dimension 28×28 , train: 60000, calibration: 1000, test: 9000.
- ImageNet 2012 [45]: Image database of natural objects and scenes. 1000 classes, train: 1.2 million, calibration: 1000, test: 9000.

Binary Classification We trained two boosting variants (AdaBoost [46, 47], XGBoost [48]), two forest variants (Mondrian Forest [49], Random Forest [50]) and a simple one layer neural network on the binary KITTI and PCam data sets. We report the average ECE_1 in Table 1. For binary problems all calibration methods perform similarly with the exception of isotonic regression, which has particularly low calibration error on the KITTI data set. However due to its piece-wise constant calibration map the resulting confidence distribution of the predicted class has a set of singular peaks instead of a smooth distribution. While GP calibration is competitive across data sets and classifiers, it does not outperform any of the other methods and is computationally more expensive. Hence, if

¹An implementation of GP calibration is available at <http://github.com/JonathanWenger/pycalib>.

Table 1: Average ECE_1 of ten Monte-Carlo cross validation folds on binary benchmark data sets.

Data Set	Model	Uncal.	Platt	Isotonic	Beta	BBQ	Temp.	GPcalib
KITTI	AdaBoost	.4301	.0182	.0134	.0180	.0190	.0185	.0192
KITTI	XGBoost	.0434	.0198	.0114	.0178	.0184	.0204	.0186
KITTI	Mondr. Forest	.0546	.0198	.0142	.0252	.0218	.0200	.0202
KITTI	Rand. Forest	.0768	.0147	.0135	.0159	.0652	.0126	.0182
KITTI	1 layer NN	.0153	.0285	.0121	.0174	.0178	.0280	.0156
PCam	AdaBoost	.2506	.0409	.0335	.0397	.0330	.0381	.0389
PCam	XGBoost	.0605	.0378	.0323	.0356	.0312	.0399	.0332
PCam	Mondr. Forest	.0415	.0428	.0291	.0349	.0643	.0427	.0347
PCam	Rand. Forest	.0798	.0237	.0233	.0293	.0599	.0210	.0285
PCam	1 layer NN	.2090	.0717	.0297	.0501	.0296	.0542	.0461

Table 2: Average ECE_1 of ten Monte-Carlo cross validation folds on multi-class benchmark data sets.

Data Set	Model	Uncal.	one-vs-all				Temp.	GPcalib
			Platt	Isotonic	Beta	BBQ		
MNIST	AdaBoost	.6121	.2267	.1319	.2222	.1384	.1567	.0414
MNIST	XGBoost	.0740	.0449	.0176	.0184	.0207	.0222	.0180
MNIST	Mondr. Forest	.2163	.0357	.0282	.0383	.0762	.0208	.0213
MNIST	Rand. Forest	.1178	.0273	.0207	.0259	.1233	.0121	.0148
MNIST	1 layer NN	.0262	.0126	.0140	.0168	.0186	.0195	.0239
ImageNet	AlexNet	.0354	.1143	.2771	.2321	.1344	.0336	.0354
ImageNet	VGG19	.0375	.1018	.2656	.2484	.1642	.0347	.0351
ImageNet	ResNet50	.0444	.0911	.2632	.2239	.1627	.0333	.0333
ImageNet	ResNet152	.0525	.0862	.2374	.2177	.1665	.0328	.0336
ImageNet	DenseNet121	.0369	.0941	.2374	.2277	.1536	.0333	.0331
ImageNet	DenseNet201	.0421	.0923	.2306	.2195	.1602	.0319	.0336
ImageNet	Inception v4	.0311	.0852	.2795	.1628	.1569	.0460	.0307
ImageNet	SE ResNeXt50	.0432	.0837	.2570	.1723	.1717	.0462	.0311
ImageNet	SE ResNeXt101	.0571	.0837	.2718	.1660	.1513	.0435	.0317

exclusively binary problems are of interest, a simple calibration method such as isotonic regression or Beta calibration should be preferred. The simple layer neural network on the KITTI data set is already well calibrated, nonetheless all calibration methods except isotonic regression and GP calibration increase the ECE_1 .

Multi-class Classification Aside the aforementioned classification models, which were trained on MNIST, we also calibrated pre-trained convolutional neural network architectures on ImageNet. The following CNNs were used: AlexNet [51], VGG19 [52], ResNet50, ResNet152 [53], DenseNet121, DenseNet201 [54], Inception v4 [55], SE ResNeXt50, SE ResNeXt101 [56, 57]. All binary calibration methods were extended to the multi-class setting in a one-vs-all manner. Temperature scaling was applied to logits for all CNNs and otherwise directly to probability scores. The average expected calibration error is shown in Table 2. While binary methods still perform reasonably well for 10 classes in the case of MNIST, they worsen calibration in the case of a 1000 classes on ImageNet. Moreover, they also skew the posterior predictive distribution so much that accuracy is sometimes severely affected, disqualifying them from use. Temperature scaling preserves the underlying accuracy of the classifier by definition. Even though GP calibration has no such guarantees, our experiments show very little effect on accuracy (see Table S2 in the supplementary material). GP calibration outperforms temperature scaling for boosting methods on MNIST. These tend to be severely underconfident and in the case of AdaBoost have low confidence overall. Only our method is able to handle this. Both temperature scaling and GP calibration perform well across CNN architectures on ImageNet. It performs particularly well on CNNs which demonstrate high accuracy. Further, in contrast to all other methods, GP calibration preserves low ECE_1 for Inception v4. We attribute this desirable behavior, also seen in the binary case, to the prior assumption that the underlying classification

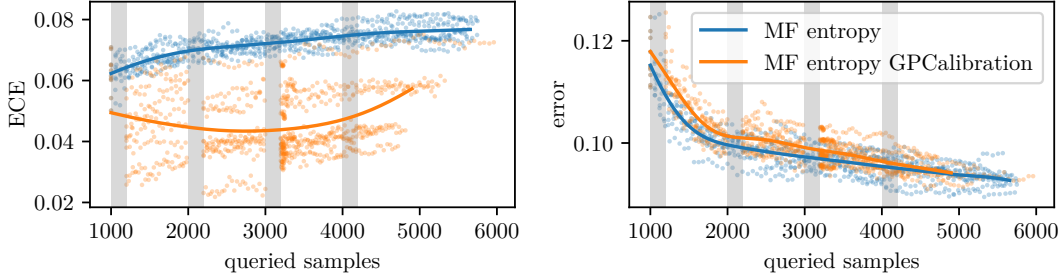


Figure 3: **Active learning and calibration.** ECE_1 and classification error for two Mondrian forests trained online on labels requested through an entropy query strategy on the KITTI data set. One Mondrian forest is calibrated at regularly spaced intervals (in gray) using GP calibration. Raw data and a Gaussian process regression up to the average number of queried samples across folds is shown.

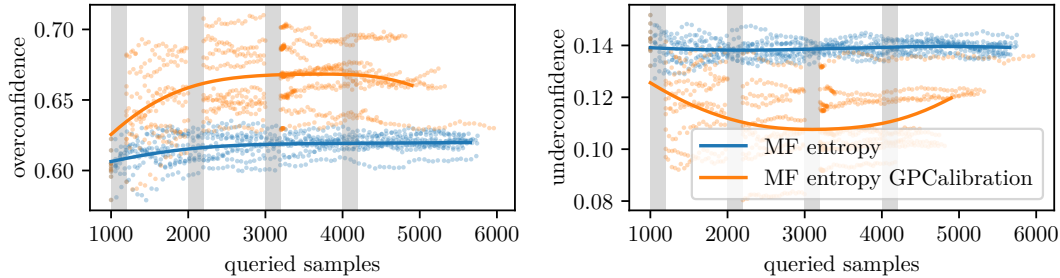


Figure 4: **Effects of calibration on over- and underconfidence in active learning.** Over- and underconfidence for two Mondrian forests trained online in an active fashion. The Mondrian forest which was calibrated in regularly spaced intervals (in gray) demonstrates a shift in over- and underconfidence to the ratio determined by Theorem 1. Raw data and a Gaussian process regression up to the average number of queried samples across folds is shown.

method is already calibrated. The increased flexibility of the non-parametric latent function and its prior assumptions allow GP calibration to better adapt to various classifiers and data sets.

Active Learning We hypothesize that a better uncertainty estimation of the posterior through calibration leads to an improved learning process when doing active learning. To evaluate this, we use the multi-class KITTI data set, for which we trained two Mondrian forests. These are particularly suited to the online setting, as they are computationally efficient to train and have the same distribution whether trained online or in batch. We randomly shuffled the data 10 times and request samples based on an entropy query strategy with a threshold of 0.5. Any samples above the threshold are used for training. Both forests are trained for 1000 samples and subsequently one uses 200 samples exclusively for calibration in regularly spaced intervals.

We report the expected calibration and classification error in Figure 3. As we can see, the calibration initially incurs a penalty on accuracy for the calibrated forest, as fewer samples are used for training. This penalty is remedied over time through more efficient querying. The same error of the uncalibrated Mondrian forest is reached after a pass through the entire data while less samples overall were requested. A look at the influence of calibration on over- and underconfidence in Figure 4 illustrates the effect of Theorem 1 and the reason for the more conservative label requests and therefore improved efficiency. Underconfidence is reduced at the expense of overconfidence leading to a more conservative sampling strategy, which does not penalize accuracy in the long run.

5 Conclusion

In this paper, we proposed a novel multi-class calibration method for arbitrary classifiers based on a latent Gaussian process, inferred through variational inference. We evaluated different calibration methods for a range of classifiers often employed in computer vision and robotics on benchmark

data sets. Further, we studied the impact of calibration on active learning. Our proposed calibration approach is worth extending in the following directions: (a) forcing a monotone latent Gaussian process (e.g. [58]) provably preserves the accuracy of the underlying classifier; (b) extending our method to the online setting (e.g. [59]) allows for continuous calibration; (c) using our method for what we call *active calibration*, the concept of using an active learning query strategy, which switches between requesting samples for model training and uncertainty calibration based on the uncertainty of the latent Gaussian process.

References

- [1] Dario Amodei, Chris Olah, Jacob Steinhardt, Paul Francis Christiano, John Schulman, and Dan Mané. Concrete problems in AI safety. *CoRR*, abs/1606.06565, 2016.
- [2] Burr Settles. Active learning literature survey. Technical Report 55-66, University of Wisconsin, Madison, 2010.
- [3] Balaji Lakshminarayanan, Alexander Pritzel, and Charles Blundell. Simple and scalable predictive uncertainty estimation using deep ensembles. In *Advances in Neural Information Processing Systems*, pages 6402–6413, 2017.
- [4] Chuan Guo, Geoff Pleiss, Yu Sun, and Kilian Q Weinberger. On calibration of modern neural networks. In *Proceedings of the 34th International Conference on Machine Learning (ICML)*, 2017.
- [5] Allan H. Murphy. A new vector partition of the probability score. *Journal of Applied Meteorology (1962-1982)*, 12(4):595–600, 1973.
- [6] Morris H. DeGroot and Stephen E. Fienberg. The comparison and evaluation of forecasters. *Journal of the Royal Statistical Society. Series D (The Statistician)*, 32(1/2):12–22, 1983.
- [7] Mahdi Pakdaman Naeini, Gregory F. Cooper, and Milos Hauskrecht. Obtaining well calibrated probabilities using bayesian binning. In Blai Bonet and Sven Koenig, editors, *Proceedings of the Twenty-Ninth AAAI Conference on Artificial Intelligence, January 25-30, 2015, Austin, Texas, USA.*, pages 2901–2907. AAAI Press, 2015.
- [8] Meelis Kull, Telmo Silva Filho, and Peter Flach. Beta calibration: a well-founded and easily implemented improvement on logistic calibration for binary classifiers. In *Proceedings of the 20th International Conference on Artificial Intelligence and Statistics*, volume 54 of *Proceedings of Machine Learning Research*, pages 623–631. PMLR, 2017.
- [9] Aviral Kumar, Sunita Sarawagi, and Ujjwal Jain. Trainable calibration measures for neural networks from kernel mean embeddings. In *Proceedings of the 35th International Conference on Machine Learning, ICML 2018, Stockholm, Sweden, July 10-15, 2018*, pages 2810–2819, 2018.
- [10] Juozas Vaicenavicius, David Widmann, Carl Andersson, Fredrik Lindsten, Jacob Roll, and Thomas Schön. Evaluating model calibration in classification. In *Proceedings of Machine Learning Research*, volume 89 of *Proceedings of Machine Learning Research*, pages 3459–3467. PMLR, 2019.
- [11] Bianca Zadrozny and Charles Elkan. Obtaining calibrated probability estimates from decision trees and naive bayesian classifiers. In *Proceedings of the 18th International Conference on Machine Learning*, pages 609–616, 2001.
- [12] Alexandru Niculescu-Mizil and Rich Caruana. Predicting good probabilities with supervised learning. In *Proceedings of the 22nd International Conference on Machine Learning*, pages 625–632. ACM, 2005.
- [13] Alexandru Niculescu-Mizil and Rich Caruana. Obtaining calibrated probabilities from boosting. In *UAI*, page 413, 2005.
- [14] David J. C. MacKay. A practical bayesian framework for backpropagation networks. *Neural Computation*, 4(3):448–472, 1992.

- [15] Yarin Gal. *Uncertainty in Deep Learning*. PhD thesis, University of Cambridge, 2016.
- [16] James Martens and Roger Grosse. Optimizing neural networks with kronecker-factored approximate curvature. In *International conference on machine learning*, pages 2408–2417, 2015.
- [17] Jimmy Ba, Roger Grosse, and James Martens. Distributed second-order optimization using kronecker-factored approximations. In *ICLR*, 2017.
- [18] Yann LeCun, Léon Bottou, Yoshua Bengio, and Patrick Haffner. Gradient-based learning applied to document recognition. In *Proceedings of the IEEE*, volume 86/11, pages 2278–2324, 1998.
- [19] Alex Kendall and Yarin Gal. What uncertainties do we need in bayesian deep learning for computer vision? In *Advances in Neural Information Processing Systems 30*, pages 5574–5584, 2017.
- [20] Gabriel Pereyra, George Tucker, Jan Chorowski, Lukasz Kaiser, and Geoffrey E. Hinton. Regularizing neural networks by penalizing confident output distributions. In *5th International Conference on Learning Representations, ICLR*, 2017.
- [21] Wesley Maddox, Timur Garipov, Pavel Izmailov, Dmitry Vetrov, and Andrew Gordon Wilson. A simple baseline for bayesian uncertainty in deep learning. *arXiv preprint arXiv:1902.02476*, 2019.
- [22] Dimitrios Miliotis, Raffaello Camoriano, Pietro Michiardi, Lorenzo Rosasco, and Maurizio Filippone. Dirichlet-based gaussian processes for large-scale calibrated classification. In *Advances in Neural Information Processing Systems 31*, pages 6008–6018, 2018.
- [23] John C. Platt. Probabilistic outputs for support vector machines and comparisons to regularized likelihood methods. In *Advances in Large-Margin Classifiers*, pages 61–74. MIT Press, 1999.
- [24] Hsuan-Tien Lin, Chih-Jen Lin, and Ruby C Weng. A note on platt’s probabilistic outputs for support vector machines. *Machine learning*, 68(3):267–276, 2007.
- [25] Bianca Zadrozny and Charles Elkan. Transforming classifier scores into accurate multiclass probability estimates. In *Proceedings of the Eighth ACM SIGKDD International Conference on Knowledge Discovery and Data Mining, KDD ’02*, pages 694–699, New York, NY, USA, 2002. ACM.
- [26] Volodymyr Kuleshov and Stefano Ermon. Estimating uncertainty online against an adversary. In *AAAI*, pages 2110–2116, 2017.
- [27] Volodymyr Kuleshov, Nathan Fenner, and Stefano Ermon. Accurate uncertainties for deep learning using calibrated regression. In *Proceedings of the 35th International Conference on Machine Learning*, volume 80 of *Proceedings of Machine Learning Research*, pages 2796–2804. PMLR, 2018.
- [28] Hao Song, Tom Diethe, Meelis Kull, and Peter Flach. Distribution calibration for regression. *Proceedings of the 36th International Conference on Machine Learning*, 2019.
- [29] Fattaneh Jabbari, Mahdi Pakdaman Naeini, and Gregory Cooper. Obtaining accurate probabilistic causal inference by post-processing calibration. In *NIPS 2017 Workshop on Causal Inference and Machine Learning*, 2017.
- [30] Geoff Pleiss, Manish Raghavan, Felix Wu, Jon Kleinberg, and Kilian Q Weinberger. On fairness and calibration. In *Advances in Neural Information Processing Systems*, pages 5680–5689, 2017.
- [31] Jon Kleinberg. Inherent trade-offs in algorithmic fairness. *SIGMETRICS Perform. Eval. Rev.*, 46(1):40–40, 2018.
- [32] Allan H. Murphy and Robert L. Winkler. Diagnostic verification of probability forecasts. *International Journal of Forecasting*, 7:435–455, 1992.

- [33] Ira Cohen and Moises Goldszmidt. Properties and benefits of calibrated classifiers. In *8th European Conference on Principles and Practice of Knowledge Discovery in Databases (PKDD)*, pages 125–136. Springer, 2004.
- [34] D. Mund, R. Triebel, and D. Cremers. Active online confidence boosting for efficient object classification. In *2015 IEEE International Conference on Robotics and Automation (ICRA)*, pages 1367–1373, 2015.
- [35] Meelis Kull, Telmo M Silva Filho, Peter Flach, et al. Beyond sigmoids: How to obtain well-calibrated probabilities from binary classifiers with beta calibration. *Electronic Journal of Statistics*, 11(2):5052–5080, 2017.
- [36] Carl Edward Rasmussen and Christopher K. I. Williams. *Gaussian Processes for Machine Learning (Adaptive Computation and Machine Learning)*. The MIT Press, 2005.
- [37] James Hensman, Alexander G. de G. Matthews, and Zoubin Ghahramani. Scalable variational gaussian process classification. In *Proceedings of AISTATS*, 2015.
- [38] David M Blei, Alp Kucukelbir, and Jon D McAuliffe. Variational inference: A review for statisticians. *Journal of the American Statistical Association*, 112(518):859–877, 2017.
- [39] Cheng Zhang, Judith Bütetpage, Hedvig Kjellström, and Stephan Mandt. Advances in variational inference. *IEEE transactions on pattern analysis and machine intelligence*, 2018.
- [40] Alexander G. de G. Matthews, Mark van der Wilk, Tom Nickson, Keisuke Fujii, Alexis Boukouvalas, Pablo Le‘on-Villagr‘a, Zoubin Ghahramani, and James Hensman. GPflow: A Gaussian process library using TensorFlow. *Journal of Machine Learning Research*, 18(40): 1–6, 2017-04.
- [41] Andreas Geiger, Philip Lenz, and Raquel Urtasun. Are we ready for autonomous driving? the kitti vision benchmark suite. In *Conference on Computer Vision and Pattern Recognition (CVPR)*, 2012.
- [42] Alexander Narr, Rudolph Triebel, and Daniel Cremers. Stream-based active learning for efficient and adaptive classification of 3d objects. In *Robotics and Automation (ICRA), 2016 IEEE International Conference on*, pages 227–233. IEEE, 2016.
- [43] Michael Himmelsbach, Thorsten Luetzel, and H-J Wuensche. Real-time object classification in 3d point clouds using point feature histograms. In *2009 IEEE/RSJ International Conference on Intelligent Robots and Systems*, pages 994–1000. IEEE, 2009.
- [44] Bastiaan S Veeling, Jasper Linmans, Jim Winkens, Taco Cohen, and Max Welling. Rotation equivariant cnns for digital pathology. In *International Conference on Medical image computing and computer-assisted intervention*, pages 210–218. Springer, 2018.
- [45] Olga Russakovsky, Jia Deng, Hao Su, Jonathan Krause, Sanjeev Satheesh, Sean Ma, Zhiheng Huang, Andrej Karpathy, Aditya Khosla, Michael Bernstein, Alexander C. Berg, and Li Fei-Fei. ImageNet Large Scale Visual Recognition Challenge. *International Journal of Computer Vision (IJCV)*, 115(3):211–252, 2015.
- [46] Yoav Freund and Robert E Schapire. A decision-theoretic generalization of on-line learning and an application to boosting. *Journal of computer and system sciences*, 55(1):119–139, 1997.
- [47] Trevor Hastie, Saharon Rosset, Ji Zhu, and Hui Zou. Multi-class adaboost. *Statistics and its Interface*, 2(3):349–360, 2009.
- [48] Tianqi Chen and Carlos Guestrin. XGBoost: A scalable tree boosting system. In *Proceedings of the 22nd ACM SIGKDD International Conference on Knowledge Discovery and Data Mining, KDD ’16*, pages 785–794. ACM, 2016.
- [49] Balaji Lakshminarayanan, Daniel M. Roy, and Yee Whye Teh. Mondrian forests: Efficient online random forests. In *Proceedings of the 27th International Conference on Neural Information Processing Systems - Volume 2, NIPS’14*, pages 3140–3148, Cambridge, MA, USA, 2014. MIT Press.

- [50] Leo Breiman. Random forests. *Machine Learning*, 45(1):5–32, 2001.
- [51] Alex Krizhevsky, Ilya Sutskever, and Geoffrey E. Hinton. Imagenet classification with deep convolutional neural networks. In *Proceedings of the 25th International Conference on Neural Information Processing Systems - Volume 1, NIPS' 12*, pages 1097–1105. Curran Associates Inc., 2012.
- [52] S. Liu and W. Deng. Very deep convolutional neural network based image classification using small training sample size. In *3rd IAPR Asian Conference on Pattern Recognition (ACPR)*, pages 730–734, 2015.
- [53] Kaiming He, Xiangyu Zhang, Shaoqing Ren, and Jian Sun. Deep residual learning for image recognition. *2016 IEEE Conference on Computer Vision and Pattern Recognition (CVPR)*, pages 770–778, 2016.
- [54] Gao Huang, Zhuang Liu, Laurens van der Maaten, and Kilian Q Weinberger. Densely connected convolutional networks. In *Proceedings of the IEEE Conference on Computer Vision and Pattern Recognition*, 2017.
- [55] Christian Szegedy, Sergey Ioffe, and Vincent Vanhoucke. Inception-v4, inception-resnet and the impact of residual connections on learning. In *AAAI*, 2016.
- [56] Saining Xie, Ross B. Girshick, Piotr Dollár, Zhuowen Tu, and Kaiming He. Aggregated residual transformations for deep neural networks. *2017 IEEE Conference on Computer Vision and Pattern Recognition (CVPR)*, pages 5987–5995, 2017.
- [57] Jie Hu, Li Shen, and Gang Sun. Squeeze-and-excitation networks. In *IEEE Conference on Computer Vision and Pattern Recognition*, 2018.
- [58] Jaakko Riihimäki and Aki Vehtari. Gaussian processes with monotonicity information. In *Proceedings of the Thirteenth International Conference on Artificial Intelligence and Statistics*, pages 645–652, 2010.
- [59] Thang D Bui, Cuong Nguyen, and Richard E Turner. Streaming sparse gaussian process approximations. In *Advances in Neural Information Processing Systems*, pages 3299–3307, 2017.

This is the supplementary material for the paper: “Non-Parametric Calibration for Classification”, by Jonathan Wenger, Hedvig Kjellström and Rudolph Triebel.

S1 Proof of Theorem 1

We provide a proof for the calibration error bound to the weighted absolute difference between over- and underconfidence in Theorem 1.

Proof. By linearity of expectation and the tower rule it holds that

$$\mathbb{E}[\hat{z}] = \mathbb{E}[\hat{z} + \mathbb{E}[1_{\hat{y}=y} | \hat{z}] - \mathbb{E}[1_{\hat{y}=y} | \hat{z}]] = \mathbb{E}[\hat{z} - \mathbb{E}[1_{\hat{y}=y} | \hat{z}]] + \mathbb{P}(\hat{y} = y).$$

Conversely, by decomposing the average confidence we have

$$\begin{aligned} \mathbb{E}[\hat{z}] &= \mathbb{E}[\hat{z} | \hat{y} \neq y] \mathbb{P}(\hat{y} \neq y) + \mathbb{E}[\hat{z} | \hat{y} = y] \mathbb{P}(\hat{y} = y) \\ &= \mathbb{E}[\hat{z} | \hat{y} \neq y] \mathbb{P}(\hat{y} \neq y) + (1 - \mathbb{E}[1 - \hat{z} | \hat{y} = y]) \mathbb{P}(\hat{y} = y) \\ &= o(f) \mathbb{P}(\hat{y} \neq y) + (1 - u(f)) \mathbb{P}(\hat{y} = y). \end{aligned}$$

Combining the above we obtain

$$\mathbb{E}[\hat{z} - \mathbb{E}[1_{\hat{y}=y} | \hat{z}]] = o(f) \mathbb{P}(\hat{y} \neq y) - u(f) \mathbb{P}(\hat{y} = y).$$

Now, since $f(x) = |x|^p$ is convex for $1 \leq p < \infty$, we have by Jensen’s inequality

$$|\mathbb{E}[\hat{z} - \mathbb{E}[1_{\hat{y}=y} | \hat{z}]]|^p \leq \mathbb{E}[|\hat{z} - \mathbb{E}[1_{\hat{y}=y} | \hat{z}]|^p]$$

and finally by Hölder’s inequality with $1 \leq p < q \leq \infty$ it follows that

$$\text{ECE}_p = \mathbb{E}[|\hat{z} - \mathbb{E}[1_{\hat{y}=y} | \hat{z}]|^p]^{\frac{1}{p}} \leq \mathbb{E}[|\hat{z} - \mathbb{E}[1_{\hat{y}=y} | \hat{z}]|^q]^{\frac{1}{q}} = \text{ECE}_q,$$

which concludes the proof. \square

S2 Inference and Prediction for GP Calibration

We give a more detailed exposition of GP calibration inference. We begin by describing the derivation of the bound on the marginal log-likelihood in (6).

S2.1 Bound on the Marginal Log-Likelihood

This subsection follows [37] and is adapted for our specific inverse link function and likelihood. Consider the following bound, derived by marginalization and Jensen’s inequality.

$$\log p(\mathbf{y} | \mathbf{u}) \geq \mathbb{E}_{p(\mathbf{f} | \mathbf{u})} [\log p(\mathbf{y} | \mathbf{f})] \quad (8)$$

We then substitute (8) into the lower bound to the evidence (ELBO) as follows

$$\begin{aligned} \log p(\mathbf{y}) &= \text{KL}[q(\mathbf{u}) \| p(\mathbf{u} | \mathbf{y})] + \text{ELBO}(q(\mathbf{u})) \\ &\geq \text{ELBO}(q(\mathbf{u})) \\ &= \mathbb{E}_{q(\mathbf{u})} [\log p(\mathbf{y}, \mathbf{u})] - \mathbb{E}_{q(\mathbf{u})} [\log q(\mathbf{u})] \\ &= \mathbb{E}_{q(\mathbf{u})} [\log p(\mathbf{y} | \mathbf{u})] - \text{KL}[q(\mathbf{u}) \| p(\mathbf{u})] \\ &\geq \mathbb{E}_{q(\mathbf{u})} [\mathbb{E}_{p(\mathbf{f} | \mathbf{u})} [\log p(\mathbf{y} | \mathbf{f})]] - \text{KL}[q(\mathbf{u}) \| p(\mathbf{u})] \\ &= \mathbb{E}_{q(\mathbf{f})} [\log p(\mathbf{y} | \mathbf{f})] - \text{KL}[q(\mathbf{u}) \| p(\mathbf{u})] \\ &= \sum_{n=1}^N \mathbb{E}_{q(f_n)} [\log p(y_n | f_n)] - \text{KL}[q(\mathbf{u}) \| p(\mathbf{u})], \end{aligned} \quad (9)$$

where $q(\mathbf{f}) := \int p(\mathbf{f} | \mathbf{u}) q(\mathbf{u}) d\mathbf{u}$ and the last equality holds by independence of the calibration data. By (5) and the rules of Gaussians we obtain

$$p(\mathbf{f} | \mathbf{u}) = \mathcal{N}(\mathbf{f} | \boldsymbol{\mu}_f + \Sigma_{f,u} \Sigma_u^{-1} (\mathbf{u} - \boldsymbol{\mu}_u), \Sigma_f - \Sigma_{f,u} \Sigma_u^{-1} \Sigma_{f,u}^\top).$$

Let $q(\mathbf{u}) = \mathcal{N}(\mathbf{u} \mid m, S)$ and $A := \Sigma_{f,u} \Sigma_u^{-1}$, then

$$q(\mathbf{f}) := \int \underbrace{p(\mathbf{f} \mid \mathbf{u})q(\mathbf{u})}_{q(\mathbf{f},\mathbf{u})} d\mathbf{u} = \mathcal{N}(\mathbf{f} \mid \boldsymbol{\mu}_f + A(m - \boldsymbol{\mu}_u), \Sigma_f + A(S - \Sigma_u)A^\top).$$

as $q(\mathbf{f}, \mathbf{u})$ is normally distributed. To compute the expectations in (9) we only need to consider the K -dimensional marginals

$$q(f_n) = \int p(f_n \mid \mathbf{u})q(\mathbf{u}) d\mathbf{u} = \mathcal{N}(f_n \mid \varphi_n, C_n).$$

S2.2 Approximation of the Expectation Terms

In order to obtain the variational objective (9) we need to compute the expected value terms for our intractable likelihood (4). To do so we use a second order Taylor approximation of

$$h(f_n) := \log p(y_n \mid f_n) = \log \frac{\exp(f_n^{y_n})}{\sum_{k=1}^K \exp(f_n^k)}$$

at $f_n = \varphi_n$. The Hessian of the log-softargmax is given by

$$D_{f_n}^2 h(f_n) = D_{f_n}^2 \log \sigma(f_n)_{y_n} = \sigma(f_n)\sigma(f_n)^\top - \text{diag}(\sigma(f_n)).$$

Note that it does not depend on y_n . We obtain by using $x^\top Mx = \text{tr}(x^\top Mx)$, the linearity of the trace and its invariance under cyclic permutations, that

$$\begin{aligned} \mathbb{E}_{q(f_n)} [\log p(y_n \mid f_n)] &= \mathbb{E}_{q(f_n)} [h(f_n)] \\ &\approx \mathbb{E}_{q(f_n)} \left[h(\varphi_n) + D_{f_n} h(\varphi_n)^\top (f_n - \varphi_n) + \frac{1}{2} (f_n - \varphi_n)^\top D_{f_n}^2 h(\varphi_n) (f_n - \varphi_n) \right] \\ &= h(\varphi_n) + \frac{1}{2} \mathbb{E}_{q(f_n)} \left[(f_n - \varphi_n)^\top (\sigma(\varphi_n)\sigma(\varphi_n)^\top - \text{diag}(\sigma(\varphi_n))) (f_n - \varphi_n) \right] \\ &= h(\varphi_n) + \frac{1}{2} \text{tr} \left[\mathbb{E}_{q(f_n)} [(f_n - \varphi_n)(f_n - \varphi_n)^\top] (\sigma(\varphi_n)\sigma(\varphi_n)^\top - \text{diag}(\sigma(\varphi_n))) \right] \\ &= \log p(y_n \mid \varphi_n) + \frac{1}{2} \text{tr} [C_n (\sigma(\varphi_n)\sigma(\varphi_n)^\top - \text{diag}(\sigma(\varphi_n)))] \\ &= \log p(y_n \mid \varphi_n) + \frac{1}{2} (\text{tr} [\sigma(\varphi_n)^\top C_n \sigma(\varphi_n)] - \text{tr} [C_n \text{diag}(\sigma(\varphi_n))]) \\ &= \log p(y_n \mid \varphi_n) + \frac{1}{2} (\sigma(\varphi_n)^\top C_n \sigma(\varphi_n) - \text{diag}(C_n)^\top \sigma(\varphi_n)), \end{aligned}$$

which can be computed in $\mathcal{O}(K^2)$ by expressing the term inside the parentheses as a double sum over K terms.

S3 Additional Experimental Results

The accuracy from the binary and multi-class experiments described in Section 4 are given in Table S1 and Table S2, respectively. For the binary experiments accuracy is mostly unaffected across classifiers and even improves in some instances. Only Bayesian Binning into Quantiles suffers from a noticeable drop in accuracy for random forests. Surprisingly, for the simple neural network all binary methods actually improve upon accuracy. In the multi-class case we see that accuracy is severely affected for binary methods extended in a one-vs-all fashion for the ImageNet data set, disqualifying them from use. Both temperature scaling and GP calibration preserve accuracy across models and data sets.

Table S1: Average accuracy of ten Monte-Carlo cross validation folds on binary benchmark data sets.

Data Set	Model	Uncal.	Platt	Isotonic	Beta	BBQ	Temp.	GPcalib
KITTI	AdaBoost	.9463	.9499	.9497	.9499	.9444	.9463	.9465
KITTI	XGBoost	.9674	.9673	.9660	.9671	.9640	.9674	.9675
KITTI	Mondr. Forest	.9536	.9539	.9523	.9532	.9439	.9536	.9536
KITTI	Rand. Forest	.9639	.9628	.9616	.9625	.8922	.9639	.9637
KITTI	1 layer NN	.9620	.9644	.9686	.9684	.9647	.9620	.9620
PCam	AdaBoost	.7586	.7609	.7644	.7610	.7638	.7586	.7588
PCam	XGBoost	.8086	.8065	.8050	.8068	.8020	.8086	.8084
PCam	Mondr. Forest	.7946	.7976	.7954	.7976	.7950	.7946	.7946
PCam	Rand. Forest	.8487	.8484	.8473	.8482	.8110	.8487	.8483
PCam	1 layer NN	.5925	.6239	.6504	.6487	.6458	.5925	.5779

Table S2: Average accuracy of ten Monte-Carlo cross validation folds on multi-class benchmark data sets.

Data Set	Model	Uncal.	one-vs-all				Temp.	GPcalib
			Platt	Isotonic	Beta	BBQ		
MNIST	AdaBoost	.7311	.6601	.6787	.6642	.6540	.7311	.7289
MNIST	XGBoost	.9333	.9330	.9312	.9331	.9274	.9333	.9333
MNIST	Mondr. Forest	.9133	.9144	.9118	.9142	.7475	.9133	.9132
MNIST	Rand. Forest	.9448	.9461	.9445	.9453	.0004	.9448	.9457
MNIST	1 layer NN	.9625	.9624	.9620	.9626	.9557	.9625	.9517
ImageNet	AlexNet	.5649	.3437	.3476	.3490	.1861	.5649	.5626
ImageNet	VGG19	.7247	.4475	.4584	.4496	.2584	.7247	.7233
ImageNet	ResNet50	.7600	.4654	.4731	.4780	.2648	.7600	.7587
ImageNet	ResNet152	.7850	.4790	.4919	.4938	.2747	.7850	.7834
ImageNet	DenseNet121	.7451	.4598	.4698	.4615	.2402	.7451	.7430
ImageNet	DenseNet201	.7702	.4754	.4804	.4823	.2583	.7702	.7707
ImageNet	Inception v4	.8000	.4939	.5060	.5051	.2610	.8000	.8009
ImageNet	SE ResNeXt50	.7914	.4865	.4999	.4965	.3154	.7914	.7890
ImageNet	SE ResNeXt101	.8021	.4963	.5111	.5040	.2525	.8021	.8018